Spatiotemporal Coupling of Vessel Cavitation and Discharge of Stored Xylem Water in a Tree Sapling[1][OPEN]

Thorsten Knipfer,[a,2] Clarissa Reyes,[a] J. Mason Earles,[a,b] Z. Carter Berry,[c] Daniel M. Johnson,[d] Craig R. Brodersen,[b] and Andrew J. McElrone[a,e,2,3]

[a]Department of Viticulture and Enology, University of California, Davis, California 95616
[b]School of Forestry and Environmental Studies, Yale University, New Haven, Connecticut 06511
[c]Schmid College of Science and Technology, Chapman University, Orange, California 92866
[d]Warnell School of Forestry and Natural Resources, University of Georgia, Athens, Georgia 30602
[e]U.S. Department of Agriculture–Agricultural Research Service, Crops Pathology and Genetics Research Unit, Davis, California 95618

Water discharge from stem internal storage compartments is thought to minimize the risk of vessel cavitation. Based on this concept, one would expect that water storage compartments involved in the buffering of xylem tensions empty before the onset of vessel cavitation under drought stress, and potentially refill after soil saturation. However, scant in vivo data exist that elucidate this localized spatiotemporal coupling. In this study on intact saplings of American chestnut (*Castanea dentata*), x-ray computed microtomography (microCT) showed that the xylem matrix surrounding vessels releases stored water and becomes air-filled either concurrent to or after vessel cavitation under progressive drought stress. Among annual growth rings, the xylem matrix of the current year remained largely water-filled even under severe drought stress. In comparison, microtomography images collected on excised stems showed that applied pressures of much greater than 0 MPa were required to induce water release from the xylem matrix. Viability staining highlighted that water release from the xylem matrix was associated primarily with emptying of dead fibers. Refilling of the xylem matrix and vessels was detected in intact saplings when the canopy was bagged and stem water potential was close to 0 MPa, and in leafless saplings over the winter period. In conclusion, this study indicates that the bulk of water stored in the xylem matrix is released after the onset of vessel cavitation, and suggests that capillary water contributes to overall stem water storage under drought but is not used primarily for the prevention of drought-induced vessel cavitation in this species.

The water transport system of woody plants can experience excessive xylem tensions in response to changing environmental conditions. It is generally assumed that water stored in capacitive tissue is sourced into the transpiration stream to buffer liquid tensions that develop inside the vessel lumen, and in turn protect vessel functionality by reducing the risk of gas emboli formation (Holbrook, 1995). Experimental data collected on intact trees using sap flow sensors suggest that the process of stem water storage-release is dynamic, where water is stored during the nighttime and is released during the daytime when transpiration and xylem tension become significant (e.g. Waring et al., 1979; Goldstein et al., 1998; Cermák et al., 2007). More recently, magnetic resonance imaging (MRI) data have provided direct evidence that water storage dynamics are tightly linked to changes in stem dimensions associated with bark shrinkage and swelling (De Schepper et al., 2012). Recent studies using frequency domain reflectometry highlighted that water storage also plays an important role in long-term maintenance of plant water balance, and that the utilization of stored water can differ between xylem regions (Hao et al., 2013; Matheny et al., 2015). Expanding on these findings, we recently used x-ray computed microtomography (microCT) to characterize the time course of tissue-specific water storage in an intact tree sapling and found that dead xylem fibers rarely refill after soil saturation, suggesting a minor role for capillary water storage in diurnal storage dynamics (*Laurus nobilis*; Knipfer et al., 2017). Stem internal water storage and related transport dynamics appear to be major components of tree hydraulic functioning under drought (McCulloh et al., 2014; Pfautsch et al., 2015), but the localized spatiotemporal

coupling of drought-induced vessel cavitation and release of stored xylem water remains to be elucidated.

In woody plants, vessels are embedded in a matrix of xylem tissue composed largely of dead cell types such as libriform fibers and/or fiber-tracheids (Esau, 1958; for details on xylem tissue fractions, see Morris et al., 2016). In contrast to living cell types that provide for storage of elastic water by cell expansion (e.g. bark and xylem parenchyma), water in dead tissue compartments is stored by capillary forces acting within the narrow lumen of these structures (Tyree and Yang, 1990; Knipfer et al., 2017). The xylem pressure required for the release of capillary water is commonly determined from water-release curves on excised plant material (Tyree and Yang, 1990; Domec and Gartner, 2002; Borchert and Pockman, 2005; Jupa et al., 2016), and these data suggest that this water release is initiated at a xylem pressure of close to 0 MPa and may no longer be available when a plant experiences drought stress. In dead cell types with extremely rigid walls (i.e. not able to expand in volume), such as dead fibers that provide for capillary water storage, a release of stored water will directly result in emptying of the lumen water, which has been shown using microCT imaging (Knipfer et al., 2017). According to published studies (as cited above), stem internal water storage under drought depends primarily on elastic water storage in living cells, but the contribution of tissue-specific storage of capillary water, particularly under excised versus in vivo (intact plant) conditions, remains to be investigated.

The goal of this study was to expand on our recent observations of tissue-specific refilling (Knipfer et al., 2017), and provide new insights into the spatiotemporal coupling between drought-induced vessel cavitation and release of stored xylem water under in vivo conditions and for different annual growth rings. Our general hypothesis was that dead tissue compartments in xylem (i.e. capillary water storage) empty during early stages of drought, and this water will be used predominantly before vessel cavitation to buffer drought-induced xylem tensions inside the vessel. We conducted our study on American chestnut (*Castanea dentata*), which can be treated as a good example of a ring porous species where vessels are embedded in a xylem matrix composed largely of fibers that can provide for water storage when filled. Using microCT, time-series imaging data were collected for stem tissue of 2-year–old intact saplings. In vivo observations were compared to water-release dynamics of the xylem matrix of excised stems. Fluorescence light microscopy was used to detect the location of metabolically active cells in the stem.

RESULTS

Vessel Cavitation and Release of Stored Water under Drought

The spatiotemporal coupling of vessel cavitation and emptying of cells in the xylem matrix was investigated in three intact *C. dentata* saplings. As shown for a representative sapling (Fig. 1), drought stress induced a decline in stem water potential (Ψ_{stem}) from -0.25 MPa to -3.0 MPa over a period of 18 h. This was linked to a reduction in stem cross-sectional area (A_{stem}) from 18.9 to 14.1 mm² primarily associated with bark shrinkage (decline in A_{bark} from 8.8 to 5.3 mm²; Fig. 1, A–C). Inside the current-year xylem, a drought-induced reduction in Ψ_{stem} from -0.25 to -0.95 MPa resulted in an increase in number of cavitated vessels (from $n = 18$ to $n = 29$) while the entire xylem matrix remained water-filled (Fig. 1, D and E). At Ψ_{stem} of -3 MPa, many more vessels were cavitated ($n = 404$) in proximity to the vascular cambium and air-filled cells occurred in some portions of the xylem matrix ($n = 353$; Fig. 1F). Inside the older xylem, a large number of cavitated vessels ($n = 178$, i.e. native embolism) were initially distributed randomly at Ψ_{stem} of -0.25 MPa, while air-filled cells of the xylem matrix ($n \approx 1300$) were mainly located in proximity to the boundary of current (second)-year xylem (Fig. 1G). At Ψ_{stem} of -0.95 MPa, vessel cavitation and water-depletion of the xylem matrix were negligible (Fig. 1H). At Ψ_{stem} of -3 MPa, many more cavitated vessels were detected mainly toward the pith ($n = 425$), which was coupled to the occurrence of air-filled cells in the xylem matrix ($n \approx 1700$; Fig. 1I). Magnified microCT images highlight how the xylem matrix of the current annual growth ring remained water-filled when vessels started to cavitate under drought stress (Fig. 1, J and K).

In vivo measurements of time courses of n = 3 *C. dentata* saplings are summarized in Figure 2: In Sapling-1, Ψ_{stem} declined from -0.3 to -3.8 MPa over a period of 15 h (Fig. 2A), and stem shrinkage, vessel cavitation, and water release from the xylem matrix were initiated almost simultaneously at Ψ_{stem} of -0.9 MPa at ~5 h into the experiment (current-year xylem in Fig. 2B and older xylem in Fig. 2C). In Sapling-2, Ψ_{stem} declined from -0.3 to -2.9 MPa over a period of 20 h (Fig. 2D). Reductions in stem cross-sectional area (A_{stem}) were observed early on during drought (Fig. 2D) and happened before vessel cavitation and water release from the xylem matrix (Fig. 2, E and F). In current-year xylem, the xylem matrix remained entirely water-filled until $t = 13$ h while some vessels started to cavitate at $t = 4$ h (Fig. 2E). At $t > 13$ h, substantial emptying of both vessels and matrix happened simultaneously. The matrix in older xylem remained largely water-filled over the time period of investigation even though most vessels were cavitated (Fig. 2F). In Sapling-3 (Fig. 1), Ψ_{stem} declined from -0.2 MPa to -3 MPa over a period of 18 h (Fig. 2G). Similar to Sapling-2, the xylem matrix surrounding vessels remained water-filled while some vessels started to cavitate in current-year xylem at $t = 3$ h (Fig. 2H). At $t = 18$ h, substantial vessel cavitation was observed, which coincided with water release from the xylem matrix. This temporal pattern was comparable in older xylem (Fig. 2I). Reductions in A_{stem} during drought-induced changes in Ψ_{stem}, as observed for Sapling-1 to -3, were

Figure 1. Time-series microCT images collected on the same stem portion of a representative intact *C. dentata* sapling subjected to drought. Water- and air-filled tissue appears in light and dark gray, respectively. A to C, Images of the stem and corresponding (D to I) segmented images showing exclusively air-filled vessels (in red) and xylem matrix (in green). Values in images are time after initiation of drought (in h), stem water potential (in MPa), and cross-sectional area (in mm²) of stem (in A to C) and air-filled vessels or xylem matrix (in D to I, number of air-filled cells in parentheses). J to K, Enlarged microCT images showing air-filled (cavitated) vessels embedded in a matrix of water-filled xylem (examples indicated by arrows; same vessels indicated by arrows in B and C). Black boxes in (B) and (C) correspond to xylem regions shown in (J) and (K); B = bark, P = pith, X = xylem.
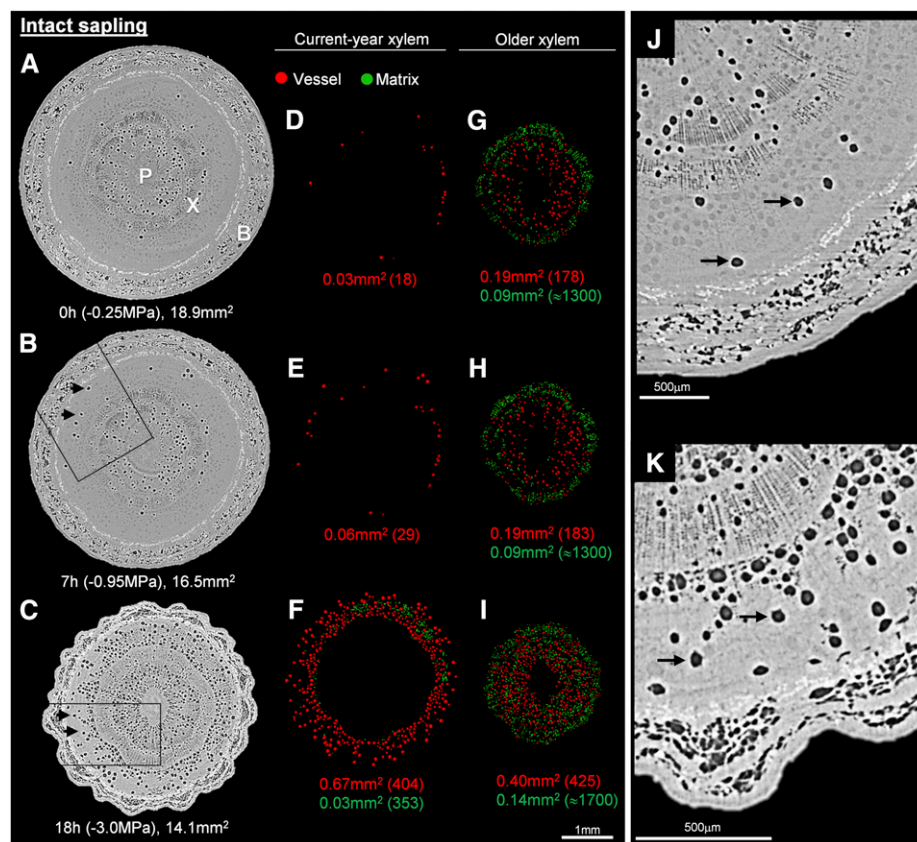
predominantly associated with bark shrinkage (see Supplemental Fig. S1).

The relationship of xylem filling status versus Ψ_{stem} shows that reductions in the water-filled cross-sectional area of the xylem matrix (i.e. discharge of stored water) did not precede vessel cavitation (Fig. 3). In current-year xylem, 50% of vessels were embolized and lost their conductivity at Ψ_{stem} of −2.2 MPa while ∼90% of A_{matrix} remained water-filled (Fig. 3). For older xylem, the presence of native embolism (Fig. 1G) did not allow us to resolve the pattern of drought-induced changes between water-filled A_{vessels} and A_{matrix}, but data showed that ∼50% of A_{matrix} remained water-filled down to Ψ_{stem} = −4 MPa. When comparing xylem regions, nonlinear regressions predicted that down to Ψ_{stem} of −2 MPa the percentage of water-filled A_{matrix} in current-year xylem remained between 90% and 100%, whereas in older xylem it decreased gradually to reach ∼75%. For Sapling-1 to -3, average A_{stem} was 20.9 ± 3.1 (SD) mm² and total A_{matrix} covered 0.60 ± 0.33 mm² of current-year xylem (= 4.4 ± 2.1 mm²) and 0.86 ± 0.22 mm² of older xylem (= 5.9 ± 2.0 mm²); total A_{vessels} was 0.53 ± 0.09 (older xylem) and 0.73 ± 0.28 (current-year) mm².

The dynamics of water release from the xylem matrix were also investigated for excised stems of *C. dentata* subjected to increasing pressure steps (Fig. 4). Changes in air-filled A_{matrix} linked to emptying of cells were negligible at applied pressures ≤0.2 MPa (Fig. 4, A, B, and E). Subsequently, the xylem matrix released water and filled progressively with air under increasingly applied pressures (Fig. 4, C–E). Images indicate a substantial increase in air-filled A_{matrix} and a radial spread toward the cambium at an applied pressure of 1 MPa (Fig. 4D). MicroCT images indicated that initial water release from excised stems (≤0.2 MPa) was associated primarily with emptying of open-ended vessels (Supplemental Fig. S2); to correct for this, water release measured at ≤0.2 MPa was assigned a negative value (Fig. 4F). Subsequently, the remaining amount of water release measured was compared to water release estimated for the xylem matrix from microCT images (Fig. 4F). At >0.2 MPa (i.e. after emptying of vessels), data indicated that the amount of water released from the xylem matrix was ∼3-times smaller as compared to measured water release, pointing to a contribution from additional tissue compartments such as living cells in bark, xylem, and pith in the excised stem (Fig. 4F).

Refilling of Xylem Vessels and Surrounding Matrix under Watered Conditions

The refilling potential of vessels and xylem matrix was investigated in stems of *C. dentata* saplings (Figs. 5 and 6; Table 1). Time-course measurements of intact saplings that were watered and with the crown covered in a humid bag, and of an excised stem that was
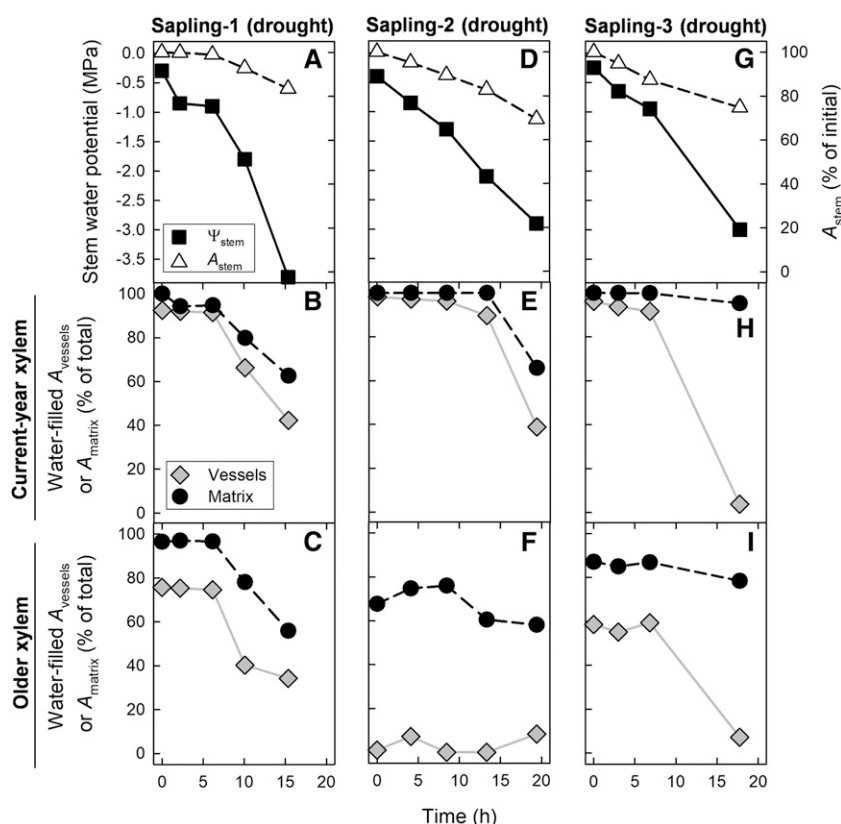
Figure 2. A to I, Time course of drought-induced changes in stem tissue of intact *C. dentata* saplings. Data were determined from transverse microCT images collected in the same stem location (as shown in Fig. 1 for Sapling-3). (Top row) Stem water potential and percentage changes in stem cross-sectional area (A_{stem}). At $t = 0$ h, initial A_{stem} was 19.2 mm^2 for Sapling-1, 24.4 mm^2 for Sapling-2, and 18.9 mm^2 for Sapling-3. (Middle and bottom rows) Percentage of cross-sectional area covered by water-filled vessels ($A_{vessels}$) or xylem matrix (A_{matrix}) in current-year and older (first year) xylem, respectively. Values on *x* axis are time after initiation of drought.

hydrated at both ends, are summarized in Figure 5: In Sapling-4, Ψ_{stem} increased from −0.3 MPa to close to 0 MPa (−0.02 MPa) over a time period of 19 h (Fig. 5A), which coincided with substantial vessel refilling and a rehydration of the xylem matrix in both current-year (Fig. 5B) and older (Fig. 5C) xylem; No reductions in A_{stem} were observed (Fig. 5A). In Sapling-5, Ψ_{stem} remained at −0.2 MPa over the time period of 17 h, and changes in A_{stem} were negligible (Fig. 5D). At the same time, no refilling of vessels and xylem matrix was detected in either current-year (Fig. 5E) or older (Fig. 5F) xylem. In the excised stem that was hydrated at both ends, again, no changes in A_{stem} were detected over the time period of investigation of 13 h (Fig. 5G) and refilling of cavitated vessels (similar to Sapling-4) was observed in both xylem rings (Fig. 5, H and I).

The refilling dynamics that occurred in one of the nontranspiring bagged saplings (Sapling-4) are shown in detail in Figure 6. In current-year xylem, $n = 28$ cavitated vessels were initially located close to the boundary between annual growth rings (Fig. 6, A and C) and almost all (93%) vessels (except for $n = 2$) appeared again water-filled at $t = 19$ h (Fig. 6, B and D; see Supplemental Fig. S3 for putative water droplets on walls of refilling vessels). In older (first year) xylem, $n = 110$ cavitated vessels and $n \approx 1,300$ water-depleted cells in the xylem matrix were present initially at $t = 0$ h (Fig. 6, A and E). At $t = 19$ h, the xylem matrix of older xylem was completely refilled while $n = 50$ vessels refilled and some cavitated vessels ($n = 60$) remained

present (Fig. 6, B and F). During this 19-h recovery period, air-voids in the bark refilled entirely (bark rehydration; Fig. 6, A and B).

Refilling of xylem vessels and matrix was also detected in leafless (nontranspiring) intact saplings during the winter period (Table 1). In Sapling-3, which was previously subjected to drought stress (Fig. 1) and then rewatered, the number of air-filled vessels and cells in the xylem matrix was reduced by >95% in current-year xylem; in older xylem, refilling was observed for vessels but not for cells in the surrounding matrix (Table 1). Similarly, refilling of vessels and xylem matrix was substantial in current-year xylem in rewatered Sapling-6 (Table 1). In Sapling-7, which had not been subjected to drought previously, the number of air-filled vessels was reduced by 68% in current-year xylem; in older xylem, a few vessels refilled and the number of air-filled cells in the matrix was reduced by 2-fold (Table 1). Together, in all three saplings refilling of xylem vessels and matrix was detected for current-year xylem, whereas refilling was less predictable in older xylem.

Anatomical Observations and Cell Viability

Tissue viability staining showed that metabolically active (living) cells in *C. dentata* stems were limited to the bark, peripheral pith tissue, and xylem parenchyma (Fig. 7). Within xylem tissue, living cells were detected
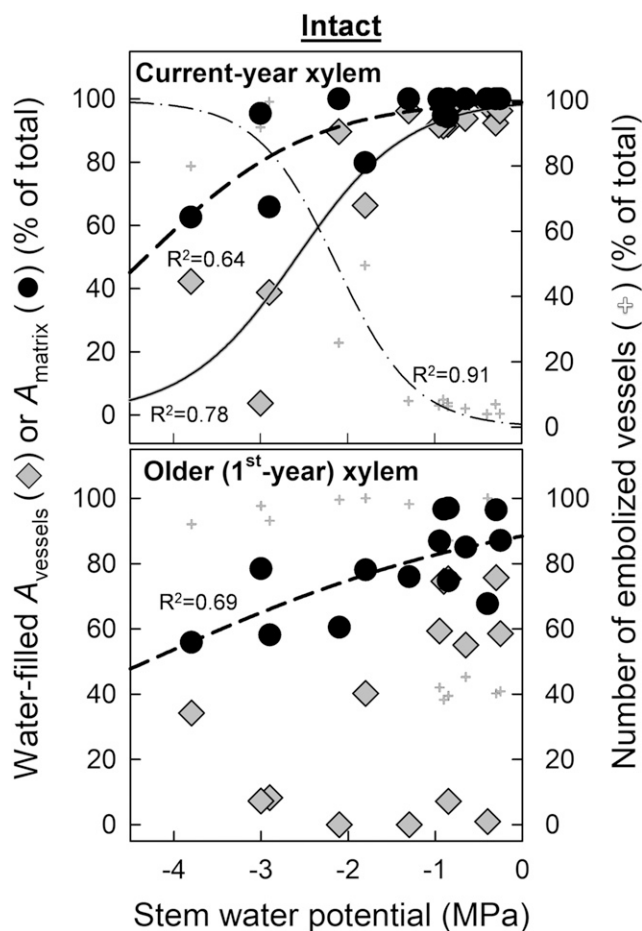
Figure 3. Relationship of drought-induced decline in Ψ_{stem} and changes in filling status of vessels and matrix in current-year and older (first year) stem xylem of intact *C. dentata* saplings. Values on *y* axis (left side) show the percentage of cross-sectional area covered by water-filled vessels and matrix; corresponding number of cavitated (embolized) vessels is shown on *y* axis on right side. Data were obtained from Saplings-1 to -3. Lines are sigmoidal nonlinear regressions shown for $P < 0.05$.

in xylem ray and in axial and paratracheal parenchyma (Fig. 7, A and B). Living cells were most abundant in current-year xylem in proximity to older xylem of the first annual growth ring (Fig. 7B, right). The amount of xylem cross-sectional area occupied by living cells was variable between stems, and estimated values ranged from 4% to 14% (older xylem) and 8% to 26% (current-year xylem). Xylem cells other than axial and paratracheal parenchyma located between rays were metabolically inactive and dead (Fig. 7C). Three-dimensional (3D) volume renderings of microCT images indicated that these dead cells were fibers (Fig. 7, D and E). In the tangential direction, xylem fibers were separated from vessels by vessel-associated paratracheal parenchyma cells (VACs) and enclosed by xylem ray parenchyma cells (Fig. 7, D and E). Fiber-to-fiber pits were present in both the tangential and radial directions, and fibers were connected to VACs (Fig. 7E).

DISCUSSION

This study on intact *C. dentata* saplings demonstrates that water stored in dead tissue compartments of the xylem matrix can contribute to overall stem water storage under drought, but based on the timing of its release, it is not used primarily for the prevention of drought-induced vessel cavitation. Time-series microCT imaging showed that vessels started to cavitate at Ψ_{stem} of ~-1 MPa, which happened simultaneously or before release of stored water from the xylem matrix. These trends were most apparent for current-year xylem (second annual growth ring), which did not have native vessel cavitation as observed in older xylem. In comparison, data collected on excised stems showed that applied pressures of $\gg 0$ MPa were required to induce water release from the xylem matrix. The magnitude to which our results extend to mature trees and other woody species needs to be investigated in future studies, but microCT images collected on *Eucalyptus camaldulensis* (Nolf et al., 2017) and *L. nobilis* (Nardini et al., 2017) show similar patterns, as found here, where the xylem matrix becomes air-filled simultaneously or after vessel cavitation. Release of water from capacitive storage compartments can aid tree hydraulic functioning under drought (McCulloh et al., 2014; Pfautsch et al., 2015), and we propose that water release from the xylem matrix under severe drought plays a negligible role in reducing the risk of vessel cavitation and is closely linked to maintenance of cambial cell viability as crucial for stress recovery and resumption of growth.

In line with findings of Bauerle et al. (2006), leaf gas exchange measurements performed on *C. dendata* saplings indicated that stomatal conductance reaches minimum values at $\Psi < -1$ MPa (Supplemental Fig. S4). This highlights that water loss by transpiration was minimal at the onset of drought-induced vessel cavitation and the release of stored xylem water from the matrix (Figs. 1 and 3). The release of water from this storage compartment occurs later in the dehydration process and is therefore more likely to be associated with maintenance of living cells near the cambium rather than providing water to the transpiration stream. We speculate that water released from dead fibers and cavitated vessels is primarily redistributed within the stem and taken up by living cells (i.e. transition from capillary to elastic storage compartment). The water release from fibers in older xylem during the winter period (Table 1), when one would expect that all compartments would refill, could be linked to such a redistribution. Typically, we observed wilting of leaves at $\Psi < -2$ MPa during a drydown (similarly, Bauerle et al. [2006] reported leaf wilting at predawn water potentials beyond -1.5 MPa) and microCT data indicate that this is the point where long-distance transport was heavily affected by vessel cavitation (i.e. 50% embolized vessels in current-year xylem; Fig. 3) and water release from the xylem matrix became significant. Together our data help to delineate the sequence of physiological
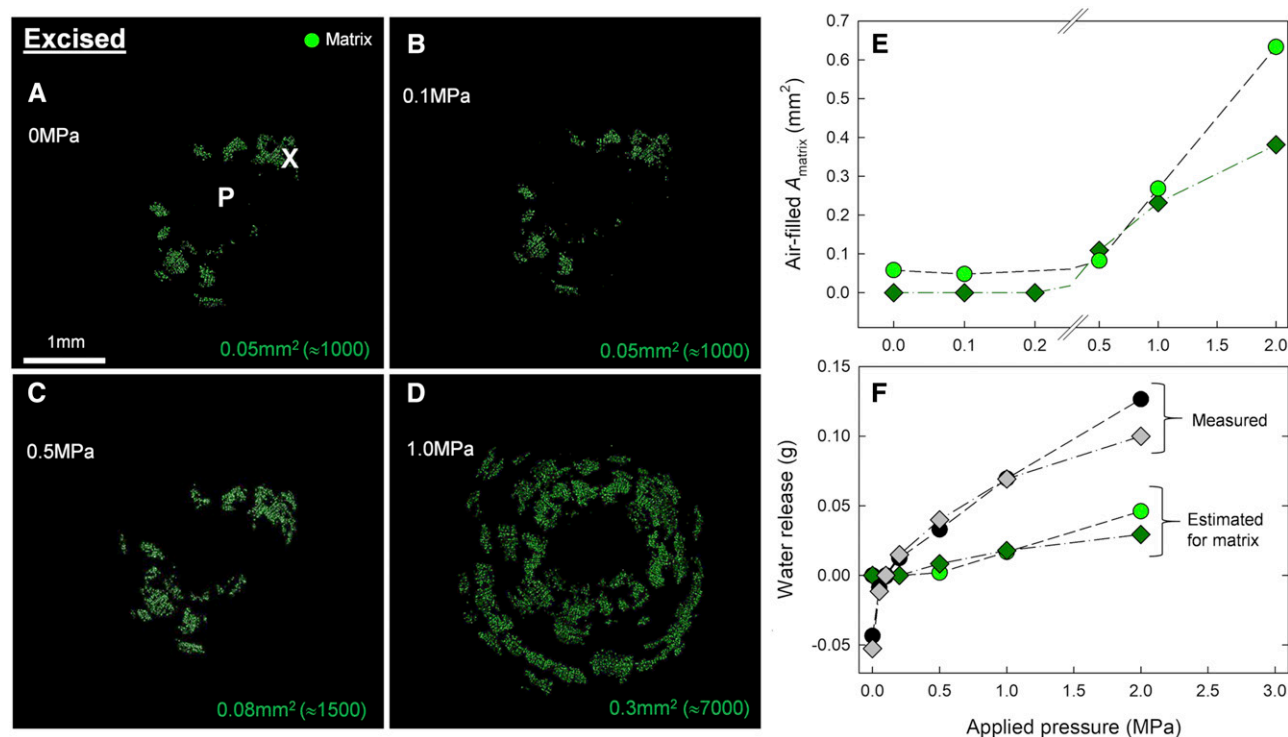
Figure 4. Water discharge from the xylem matrix as measured on an excised *C. dentata* stem subjected to increasing pressure steps. A to D, Air-filled cells in the xylem matrix are visualized in green (see Supplemental Fig. S2 for corresponding microCT images). Values in images are applied pressure to the stem end (in MPa) and cross-sectional area of air-filled xylem matrix (in mm², number of air-filled cells in parentheses; *P* = pith, *X* = xylem). Stem length and diameter were 8 cm and 4.8 mm, respectively. E, Relationship of applied pressure and cross-sectional area of air-filled xylem matrix (A_{matrix}). Different symbols represent different excised stem segments (circle symbols correspond to A to D). F, Amount of water release (in g water) measured on excised stems and corresponding amount of water release estimated from microCT images for the xylem matrix (= air-filled A_{matrix} × stem length for 1 cm³ = 1 g). The first phase (from 0 to 0.1 MPa) of the measured water release curve was dominated by vessel emptying (see Supplemental Fig. S2) and was subtracted from the curve (as indicated by negative values on *y* axis).

events related to vessel cavitation, release of stored xylem water, and stomata closure in *C. dentata* subjected to drought.

Water can be stored in dead and living portions of stem tissue (Tyree and Yang, 1990; Jupa et al., 2016; Knipfer et al., 2017). Our analysis of *C. dentata* stem xylem showed that living xylem cells only occupied up to 26% of cross-sectional area and the largest fraction of the xylem matrix surrounding vessels was metabolically inactive and dead (Fig. 7). Three-dimensional anatomical analyses indicated that this matrix was composed of fibers interconnected via pits in the tangential and radial directions (Fig. 7E). In addition, this fiber network was separated from the vessel lumen by a symplastic barrier in the presence of VACs. Recently, Morris et al. (2018) highlighted that VACs can fulfill highly specialized tasks such as controlling water movement in/out of a vessel and pathogen defense, but it remains unknown what role VACs are playing in affecting the dynamics of fiber and vessel emptying. In general, it can be assumed that a release of stored water from a dead fiber to a vessel is only possible if air (or water vapor) is able to enter the fiber lumen first (otherwise a vacuum would be generated in the empty

lumen). Air-seeding in vessels is associated with pit membrane characteristics (for review, see Choat et al., 2008), and the same would apply for cavitation (emptying) of dead xylem fibers too. Hence, the following scenario can be assumed: The propagation of a substantial liquid tension from a vessel to fibers is inhibited by VACs that are acting like a "hydraulic seal" (i.e. vessels and fibers are not directly connected). In turn, when the pressure of the vessel liquid drops to more negative values, the liquid pressure in fibers will remain at a similar level and high enough to prevent air-entry into the fiber lumen through pits (i.e. no release of stored water). Under more severe drought, the vessel cavitates but fibers in the xylem matrix will remain water-filled because the drop in liquid pressure is negligible in fibers (similar to the pattern observed in this study). This propagation of pressure between the vessel and fibers may be time-dependent, causing either a large or small pressure differential between both compartments. Therefore, a slow drydown may result in air-entry into the fiber lumen and emptying before vessel cavitation (opposite to the pattern observed in this study), and vice versa during a fast drydown. However, if pit membranes with relatively small pores

Figure 5. Time course of xylem refilling in *C. dentata*. A to F, Refilling of stem tissue in intact saplings when the soil was saturated and the crown was bagged. Data were obtained from transverse microCT images as shown in Figure 6 for Sapling-4. G and I, Refilling monitored for an excised stem segment supplied with water to both stem ends. (Top row) Stem water potential and changes in stem cross-sectional area. At $t = 0$ h, initial A_{stem} was 13.3 mm^2 for Sapling-4, 19.2 mm^2 for Sapling-5, and 10.5 mm^2 for excised stem segment. (Middle and bottom rows) Percentage of cross-sectional area covered by water-filled vessels or xylem matrix in current-year and older (first-year) xylem, respectively.
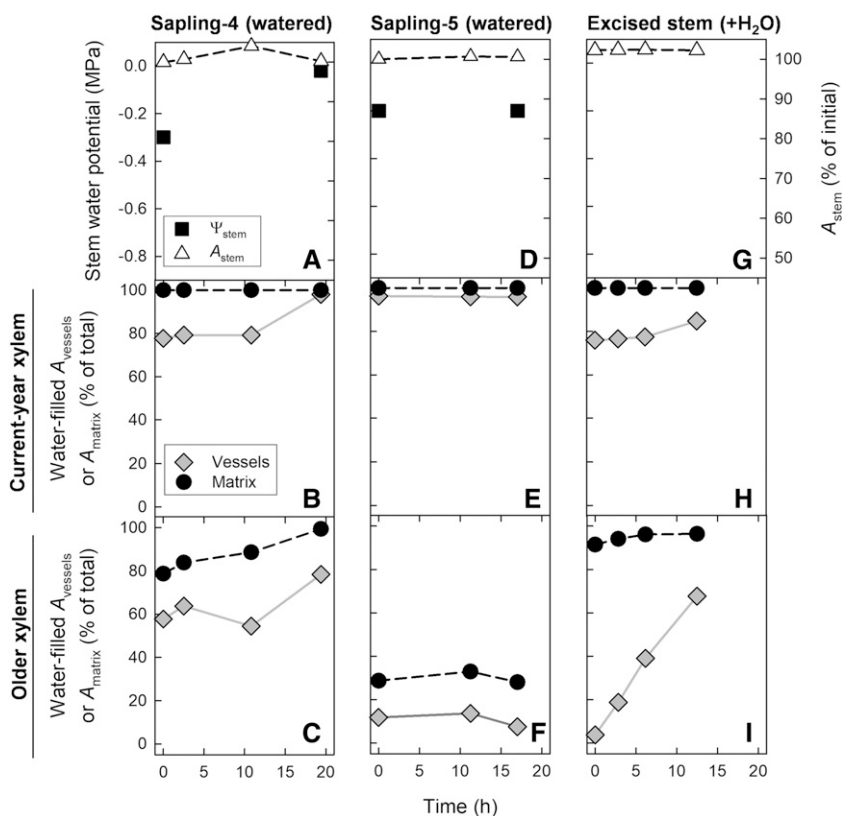

are present in fibers, then the liquid pressure in the fiber will be able to reach considerably negative values before air enters the lumen (no water release). In this case, vessels will cavitate before or simultaneously with the release of stored water from fibers even during slow (days) drying rates of the soil (similar to the pattern observed in this study). Along these lines, it has been reported that some tissue compartments for water storage in leaves are hydraulically compartmentalized and largely disconnected from the transpiration stream (Blackman and Brodribb, 2011). Future efforts should be directed at detailed 3D anatomical and functional analysis of localized transport resistances, including functional properties of fiber pits (e.g. in older versus current-year xylem), to resolve the mechanisms affecting localized flow dynamics between vessels and fibers in the intact plant.

The xylem pressure required to induce tissue-specific release of stored water can be determined on excised stems using hydraulic methods, and the capacitance for capillary and elastic water storage can be derived from the shape of measured curves (e.g. Tyree and Yang, 1990; Borchert and Pockman, 2005; Jupa et al., 2016). According to Tyree and Yang (1990), the measured curve on excised samples may be divided into three phases associated with exclusively capillary water release (phase-1), a mixture of water release from cavitated vessels, living cells and capillary water (phase-2), and predominantly elastic water release from living cells (phase-3). Data indicate that applied pressures of

close to zero are typically sufficient to induce a release of capillary water, but the required pressure can vary between species and organ types (Tyree and Yang, 1990; Jupa et al., 2016). MicroCT data collected on excised stems allowed us to directly observe the emptying of capillary storage compartments in the xylem matrix surrounding vessels. Our data indicated that release of capillary water from the xylem matrix is not initiated until pressure exceeds 0.2 MPa in *C. dentata* (Fig. 4). In the intact *C. dentata* saplings, water loss from the xylem matrix surrounding vessels was initiated mainly at Ψ_{stem} below -1.0 MPa (Figs. 2 and 3). In fact, the matrix of current-year xylem, as opposed to older xylem, remained hydrated for longer under severe drought stress (Fig. 3), which may be crucial to maintain cambial cell activity under drought and related to a higher abundance of living cells. Along these lines, measurements of Blackman and Brodribb (2011) showed that water can be stored either as "mobile" or "immobile" water in leaves, depending on the site of tissue-specific storage, and measures of capacitance on excised samples did not allow to distinguish between these water sources and did not provide a true estimate of stored water used by the intact plant.

The water transport system in a tree stem can resemble a complex network of hydraulic pathways (Siau, 1984), and a drought-induced spread of embolism has been observed for different woody species in vivo (grapevine [*Vitis vinifera*], Brodersen et al., 2013; redwood [*Sequoia sempervirens*], Choat et al., 2015; and
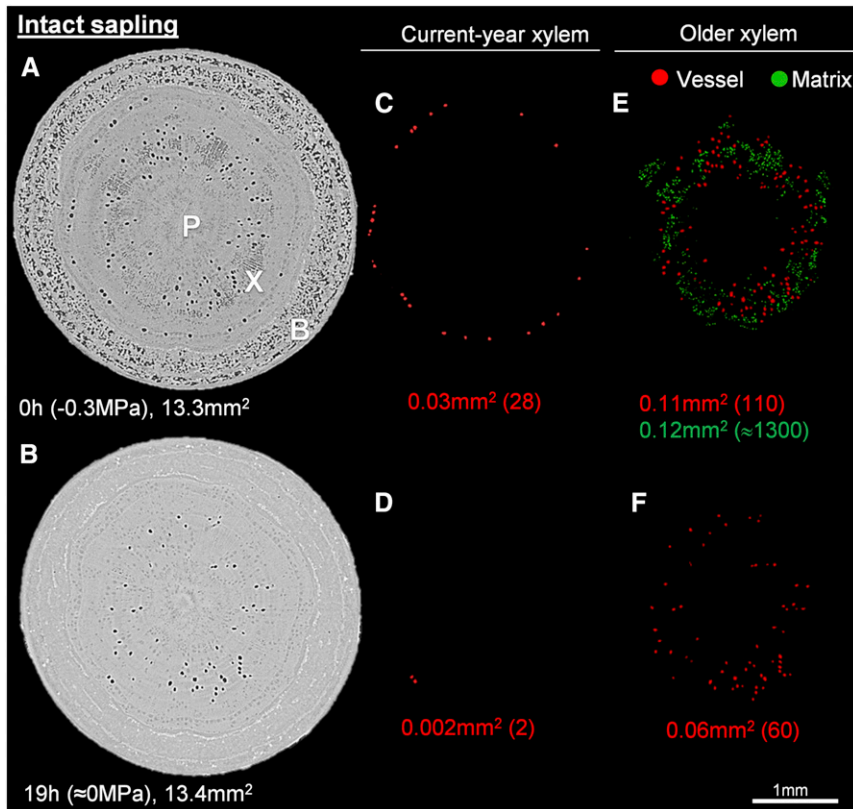
Figure 6. Time-series microCT images of the same stem portion collected for an intact *C. dentata* sapling maintained watered (soil saturated) with the crown bagged at $t = 0$ h. Water- and air-filled tissue appear in light and dark gray, respectively. A and B, Images of the stem and corresponding (C to F) segmented images showing exclusively air-filled vessels (in red) and xylem matrix (in green). Values in images are time after initiation of experiment (in h), stem water potential (in MPa), and cross-sectional area (in mm^2) of stem (in A to B) and air-filled vessels or xylem matrix (in C–F, number of air-filled cells in parentheses; B = bark, P = pith, X = xylem).

walnut [*Juglans*], Knipfer et al., 2015). Less data exists on the spatiotemporal coupling of tissue-specific water release from storage compartments. For intact *C. dentata* saplings, we found that embolism spread was initiated from the boundary of xylem annual growth rings and that this spread was not directly coupled in time to water depletion of the xylem matrix. Spatially, our data suggest that tissue connectivity is limited between annual growth rings and the transition zone between annual growth rings seems to provide a barrier minimizing the spread of air from older into current-year xylem either among vessels or matrix; a similar strategy was found in redwood xylem (Choat et al., 2015).

Bark tissue is known to release and replenish stored water on a short-term (diurnal) basis (De Schepper et al., 2012). In a recent review, Pfautsch et al. (2015) highlight the existence of a functional link between inner bark and xylem tissue via radial ray parenchyma that seems to play a crucial role in facilitating the exchange of water and carbohydrates. We detected substantial bark shrinkage during increasing drought stress and refilling of this tissue upon rewatering. In-vivo bark shrinkage was typically initiated at water potentials less negative than those resulting in water depletion of the xylem matrix and vessel cavitation, suggesting that water stored in bark was redistributed via living ray parenchyma inwards toward xylem to

Table 1. *Changes in number of air-filled xylem vessels and xylem fibers in the stem of intact* C. dentata *saplings during the winter period*

After the initial microCT scan in September, saplings were maintained well-watered and subjected to a rescan after 5 months. Saplings dropped their leaves during the winter period at the beginning of December (i.e. nontranspiring). Sapling-3 (Fig. 1) and -6 were initially subjected to drought stress (Ψ_{stem} at -3.0 MPa and -2.1 MPa, respectively); Sapling-7 was not subjected to drought.

Sample	Xylem Region	No. of Air-Filled Vessels		No. of Air-Filled Fibers	
		Initial	After 5 Months	Initial	After 5 Months
Sapling-3	Current-year	404	2	353	0
	Older	425	110	1,762	3,478
Sapling-6	Current-year	187	5	846	0
	Older	301	679	2,467	5,806
Sapling-7	Current-year	38	12	0	0
	Older	326	305	6,400	2,863

Figure 7. Stem viability and anatomy of tissue in *C. dentata* saplings. A and B, Transverse fluorescence images collected from two different saplings after staining with FDA/PI solution (left), and corresponding binary images showing exclusively metabolically active cells in older xylem (middle) and current-year xylem (right). Values in images are the estimated percentage of xylem cross-sectional area covered by living cells. C, Enlarged image of older xylem (sample in A) highlighting the presence of dead (fiber) cells (example indicated by arrow) between xylem ray parenchyma and in proximity to a vessel. B = bark, P = pith, X = xylem. D and E, Visualization of xylem anatomical features using microCT imaging. Longitudinal slice through a portion of the stem in the tangential direction (in D) and corresponding 3D volume rending (in E). Yellow box in (D) indicates portion shown. Black and white triangle indicates the presence of fiber-to-fiber pits in radial and tangential direction, respectively. Arrow indicates a connection between fiber and VAC. *f* = fiber, *V* = vessel, *RP* = xylem ray parenchyma cell.
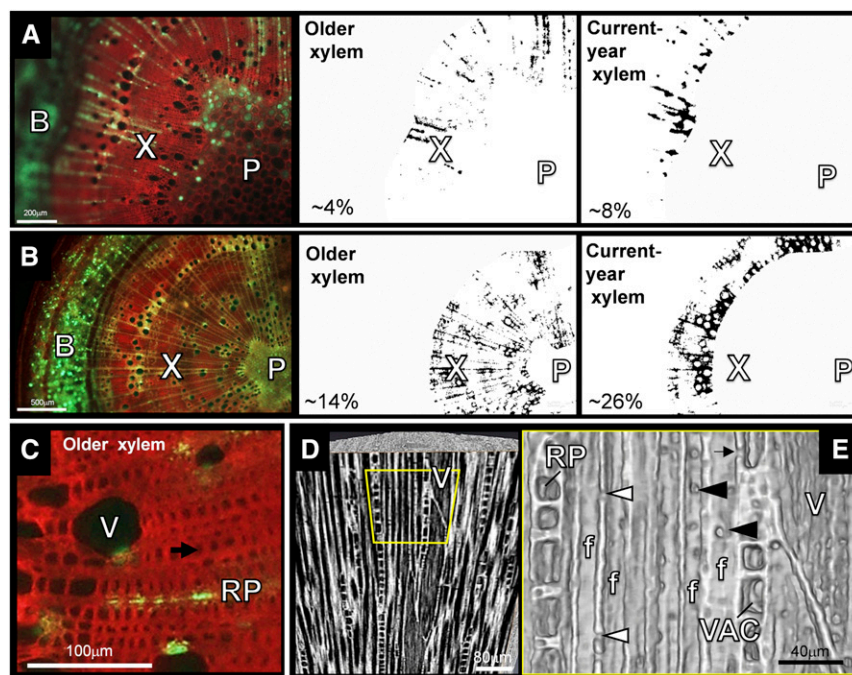
buffer drought-induced liquid tensions and minimize the risk of hydraulic failure early during drought. It may be that some water also exited the stem by bark surface evaporation, but this amount was most likely negligible because internal gradients in water potential preferentially drive water movement away from bark toward the xylem. In addition, we observed that under severe drought ($\Psi_{stem} < -1$ MPa) the cross-sectional area occupied by air voids in bark increased substantially (Fig. 1), and we assume that this phenomenon was linked to drought-induced cell dehydration. Stem and specifically bark shrinkage were not observed in watered saplings during time-series microCT imaging, indicating that the observed shrinkage was not related to multiple x-ray exposure.

In a recent study on *L. nobilis* saplings we showed that vessel and storage compartments for capillary water rarely refill in an intact plant and only if xylem tensions approach zero (Knipfer et al., 2017). Other researchers also provided experimental evidence that vessel refilling requires xylem pressures of ≥ 0 MPa (Hacke and Sperry, 2003; Charrier et al., 2016). A similar refilling phenomenon of vessel and dead xylem matrix was observed here for intact *C. dentata* saplings (see Figs. 5 and 6). Refilling of both xylem compartments was only observed in Sapling-4, where xylem pressure (i.e. Ψ_{stem}) recovered and reached a value of -0.02 MPa, close to zero (similar to *L. nobilis*; Knipfer et al., 2017). On the other hand, when xylem pressure remained at < -0.1 MPa, no refilling was induced, suggesting that internal xylem pressures were still too negative (e.g. in Sapling-5). Even though some of our refilling data were collected for well-watered saplings with native embolism, the same principle would apply for previous drought-stressed saplings after soil rewatering assuming that the activity of cells involved in

the refilling process (e.g. vessel-associated paratracheal parenchyma) fully recovers. Variations between saplings in refilling action may be associated with differences in root water uptake and subsequent rehydration of the stem, which remained unknown to us. Our observation of long-term refilling in leafless (nontranspiring) intact saplings supports our findings on short-term refilling in saplings with bagged crowns (nontranspiring). Overall, it can be concluded that refilling in an intact tree can take place under environmental conditions when transpiration from a wet or leafless canopy is negligible and the soil is saturated, allowing for negligible xylem tensions within the stem on a localized level. The success of refilling is therefore strongly dependent on a unique combination of several factors such as a plant's xylem anatomy (network connectivity and presence of living vessel-associated cells; Holbrook and Zwieniecki, 1999; Knipfer et al., 2016), the relative contribution of passive (i.e. capillarity) and active (i.e. living cells) mechanisms that drive the refilling process, and its growing environment.

MATERIALS AND METHODS

Plant Material

Water Status

Stem water potential (Ψ_{stem}) of intact saplings was measured with a Scholander Pressure Chamber (Plant Moisture Stress model 1505D; PMS

X-Ray Microtomography

Plant material was scanned using microCT (Beamline 8.3.2) at the Advance Light Source, Lawrence Berkley National Laboratory (Knipfer et al., 2017). For visualization of stem tissue, an intact sapling was placed in an aluminum cage and the same stem portion at 2–3 cm above the soil was scanned. For $n = 3$ saplings, the soil was removed from the root system immediately after the initial scan allowing for a rapid dry-down. This was necessary to reach a wide range of stress levels within the time period available for scanning, because soil water loss by transpiration was not sufficient. For $n = 2$ saplings, the soil was maintained fully saturated during the time period of investigation and the crown (including leaves and stem) was covered with a sealed plastic bag containing a wet paper towel (i.e. minimize transpiration to allow Ψ_{stem} to approach zero, similar to Knipfer et al., 2017 for *Laurus nobilis*). For each sapling, the same stem portion was scanned every couple of hours over a total time period of ~20 h. To test for long-term refilling, $n = 3$ saplings (including Sapling-3) were scanned initially in September and subsequently maintained well-watered for 5 months under atmospheric conditions; in January, approximately the same stem portion was subjected to a rescan. After completion of imaging of an intact sapling, the scanned stem portion was extracted, dried at 30°C for 5 d, and rescanned for further evaluation of tissue characteristics.

Using microCT imaging, stem tissue was also investigated in $n = 4$ excised stems obtained from saplings. The purpose of experiments on excised stems was to compare the dynamics of (1) water release from capillary storage compartments in the xylem matrix after pressurization with water release in intact saplings subjected to drought stress and (2) refilling of xylem matrix and vessels after release of xylem tensions with refilling of nontranspiring (bagged or leafless) intact saplings. A stem segment (~80 mm in length) was extracted from the intact sapling under water to minimize air aspiration during cutting with pruning shears, and stem ends were cut back with a fresh razor blade under water by ~3 mm. To study water release from xylem matrix, the stem segment was inserted into a Scholander Pressure Chamber (Plant Moisture Stress model 1505D; PMS Instrument) with the upper distal stem end protruding through the lid. The air pressure in the chamber was increased above atmospheric and maintained for ~2 min at the target pressure while water exiting the stem end was wiped off with a paper towel. When no more water exited the stem at a given pressure step, the stem was removed from the chamber and weighed. The corresponding amount of water release (in g water) was determined by initial stem weight minus stem weight at set pressure. To study xylem refilling in an excised stem, both stem ends were connected to silicone tubing that was filled with water before the initial scan (as described in Knipfer et al., 2017). For scanning, excised stems were placed in a drill chuck and scanned in the center of the stem portion.

Stems were scanned in a 21-keV synchrotron x-ray beam using a continuous tomography setting yielding 1,025 two-dimensional longitudinal images (resolution of 3.22 μm/pixel), which were captured on a complementary metal-oxide semiconductor (CMOS) camera (PCO.edge; PCO) at 350 ms exposure time. 3D stem anatomy was studied on dry stem samples scanned at 0.96-μm/pixel resolution. Acquired raw images were reconstructed into transverse images using a custom software plugin for the image-processing software FIJI (www.fiji.sc; ImageJ) that was developed at the Advance Light Source (Lawrence Berkley National Laboratory, Beamline 8.3.2) and used the software Octopus (ver. 8.3; National Institutes for Nuclear Science) in the background (Knipfer et al., 2016, 2017). Longitudinal images were generated using the "slice" tool in the software AVIZO (ver. 6,2; Visualization Sciences Group/FEI). For 3D visualization, the "volume rendering" tool in AVIZO was used.

For quantitative image analysis, stem tissue was segmented into its components of bark (including the vascular cambium because it was not possible to accurately distinguish among cambial, phloem, and peridermal tissue), current-year xylem, older (first year) xylem, and pith using the "Image-Polygon selection" tool in the software FIJI. Subsequently, air-filled portions were extracted using the "Image-Threshold" tool. Cross-sectional areas of air-filled tissue were measured using the "Analyze Particle" tool (subscript "air"); the number of air-filled cells was estimated using the same tool. Details on this image segmentation procedure can be found in Knipfer et al. (2017). For visualization of exclusively air-filled vessels and xylem matrix, a composed two-color image was generated from segmented images using the "Image Calculator" tool and the "Lookup Tables–Red/Green" tool, after using the "Process–Math–Macro" tool

to assign a grayscale value of 100 and 255 to segmented air-filled vessels and matrix, respectively. To determine the total cross-sectional area of xylem vessels and xylem matrix (subscript "total"), corresponding scans of dry stems were subjected to the same image segmentation procedure. A correction factor (α) was introduced to correct for changes in dimensions between intact versus dry stems for current-year and older xylem (= $A_{xylem\text{-}intact}/A_{xylem\text{-}dry}$). Subsequently, the percentage of cross-sectional area occupied by water-filled vessels ($A_{vessels}$) and xylem matrix (A_{matrix}) was determined according to ([$A_{total\text{-}vessels}$ $\times \alpha - A_{air\text{-}vessels}]/[A_{total\text{-}vessels} \times \alpha]) \times 100\%$ and ([$A_{total\text{-}matrix} \times \alpha - A_{air\text{-}matrix}]/$ [$A_{total\text{-}matrix} \cdot \alpha]) \times 100\%$, respectively.

Fluorescein-Diacetate–Propidium Iodide Viability Staining

Stem tissue viability was analyzed using a fluorescence-based staining assay (Knipfer et al., 2017). Two fluorescent dyes (fluorescein-diacetate [FDA] and propidium iodide [PI]) were used simultaneously that allow a two-color discrimination between living and dead cells. The FDA-PI staining solution was prepared by adding 8 μL of FDA and 50 μL of PI to 5 mL of water. Stem sections were cut free-hand using a fresh razor blade. Subsequently, sections were submerged in the staining solution for 30 min and incubated in the dark at ~23°C. Samples were mounted on a glass slide and viewed under fluorescent light (excitation filter 490 nm and 575 nm, dichromatic mirror 505 nm, barrier filter 525 nm and 625 nm) using a DM4000 B LED microscope (Leica) equipped with a DFC7000 T 2.8 MP camera (Leica). Images were captured in <4 h after sample preparation. For quantitative analysis of fluorescence images (similar to microCT image processing), stem tissue was segmented into current-year xylem and older xylem using the "Image-Polygon selection" tool in FIJI. Images were converted into 8-bit grayscale images and living portions of tissue were extracted using the "Image-Threshold" tool. Cross-sectional areas of total xylem and living xylem tissue were measured using the "Analyze Particle" tool and the living xylem parenchyma tissue fraction (as percentage of total) was determined by ($A_{living}/A_{xylem}) \times 100\%$.

Supplemental Data

The following supplemental materials are available.

Supplemental Figure S1. Relationship of drought-induced changes in A_{stem} and corresponding changes in dimensions of bark including vascular cambium, current-year (xylem second), and older (xylem first) xylem.

Supplemental Figure S2. Transverse microCT images collected on an excised stem subjected to different applied pressure steps.

Supplemental Figure S3. Longitudinal image slice through current-year xylem of Sapling-4 showing an example of a refilling vessel exhibiting a water droplet on the lateral vessel wall.

Supplemental Figure S4. Drought-induced changes in stomatal conductance.

LITERATURE CITED

Bauerle WL, Wang CG, Bowden JD, Hong CM (2006) An analysis of ecophysiological responses to drought in American Chestnut. Ann For Sci **63:** 833–842

Blackman CJ, Brodribb TJ (2011) Two measures of leaf capacitance: Insights into the water transport pathway and hydraulic conductance in leaves. Funct Plant Biol **38:** 118–126

Borchert R, Pockman WT (2005) Water storage capacitance and xylem tension in isolated branches of temperate and tropical trees. Tree Physiol **25:** 457–466

Brodersen CR, McElrone AJ, Choat B, Lee EF, Shackel KA, Matthews MA (2013) In vivo visualizations of drought-induced embolism spread in *Vitis vinifera*. Plant Physiol **161:** 1820–1829

Cermák J, Kucera J, Bauerle WL, Phillips N, Hinckley TM (2007) Tree water storage and its diurnal dynamics related to sap flow and changes in stem volume in old-growth Douglas-fir trees. Tree Physiol **27:** 181–198

Charrier G, Torres-Ruiz JM, Badel E, Burlett R, Choat B, Cochard H, Delmas CE, Domec JC, Jansen S, King A, et al (2016) Evidence for hydraulic vulnerability segmentation and lack of xylem refilling under tension. Plant Physiol **172:** 1657–1668

Choat B, Cobb AR, Jansen S (2008) Structure and function of bordered pits: New discoveries and impacts on whole-plant hydraulic function. New Phytol **177:** 608–625

Choat B, Brodersen CR, McElrone AJ (2015) Synchrotron x-ray micro-tomography of xylem embolism in *Sequoia sempervirens* saplings during cycles of drought and recovery. New Phytol **205:** 1095–1105

De Schepper V, van Dusschoten D, Copini P, Jahnke S, Steppe K (2012) MRI links stem water content to stem diameter variations in transpiring trees. J Exp Bot **63:** 2645–2653

Domec JC, Gartner BL (2002) How do water transport and water storage differ in coniferous earlywood and latewood? J Exp Bot **53:** 2369–2379

Esau K (1958) Plant Anatomy. J. Wiley and Sons, New York

Goldstein G, Andrade JL, Meinzer FC, Holbrook NM, Cavelier J, Jackson P, Celis A (1998) Stem water storage and diurnal patterns of water use in tropical forest canopy trees. Plant Cell Environ **21:** 397–406

Hacke UG, Sperry JS (2003) Limits to xylem refilling under negative pressure in *Laurus nobilis* and *Acer negundo*. Plant Cell Environ **26:** 303–311

Hao G-Y, Wheeler JK, Holbrook NM, Goldstein G (2013) Investigating xylem embolism formation, refilling and water storage in tree trunks using frequency domain reflectometry. J Exp Bot **64:** 2321–2332

Holbrook NM (1995) Stem water storage. *In* BL Gartner, ed, Plant Stem: Physiology and Functional Morphology. Academic Press, San Diego

Holbrook NM, Zwieniecki MA (1999) Embolism repair and xylem tension: Do we need a miracle? Plant Physiol **120:** 7–10

Jupa R, Plavcová L, Gloser V, Jansen S (2016) Linking xylem water storage with anatomical parameters in five temperate tree species. Tree Physiol **36:** 756–769

Knipfer T, Eustis A, Brodersen C, Walker AM, McElrone AJ (2015) Grapevine species from varied native habitats exhibit differences in embolism formation/repair associated with leaf gas exchange and root pressure. Plant Cell Environ **38:** 1503–1513

Knipfer T, Cuneo IF, Brodersen CR, McElrone AJ (2016) In situ visualization of the dynamics in xylem embolism formation and removal in the absence of root pressure: A study on excised grapevine stems. Plant Physiol **171:** 1024–1036

Knipfer T, Cuneo IF, Earles JM, Reyes C, Brodersen CR, McElrone AJ (2017) Storage compartments for capillary water rarely refill in an intact woody plant. Plant Physiol **175:** 1649–1660

Matheny AM, Bohrer G, Garity SR, Morin TH, Howard CJ, Vogel CS (2015) Observations of stem water storage in trees of opposing hydraulic strategies. Ecosphere **6:** 1–13

McCulloh KA, Johnson DM, Meinzer FC, Woodruff DR (2014) The dynamic pipeline: Hydraulic capacitance and xylem hydraulic safety in four tall conifer species. Plant Cell Environ **37:** 1171–1183

Morris H, Plavcová L, Cvecko P, Fichtler E, Gillingham MA, Martínez-Cabrera HI, McGlinn DJ, Wheeler E, Zheng J, Ziemińska K, et al (2016) A global analysis of parenchyma tissue fractions in secondary xylem of seed plants. New Phytol **209:** 1553–1565

Morris H, Plavcová L, Gorai M, Klepsch MM, Kotowska M, Jochen Schenk H, Jansen S (2018) Vessel-associated cells in angiosperm xylem: Highly specialized living cells at the symplast-apoplast boundary. Am J Bot **105:** 151–160

Nardini A, Savi T, Losso A, Petit G, Pacilè S, Tromba G, Mayr S, Trifilò P, Lo Gullo MA, Salleo S (2017) X-ray microtomography observations of xylem embolism in stems of *Laurus nobilis* are consistent with hydraulic measurements of percentage loss of conductance. New Phytol **213:** 1068–1075

Nolf M, Lopez R, Peters JMR, Flavel RJ, Koloadin LS, Young IM, Choat B (2017) Visualization of xylem embolism by x-ray microtomography: A direct test against hydraulic measurements. New Phytol **214:** 890–898

Pfautsch S, Hölttä T, Mencuccini M (2015) Hydraulic functioning of tree stems—fusing ray anatomy, radial transfer and capacitance. Tree Physiol **35:** 706–722

Siau JF (1984) Transport Processes in Wood. Springer, Berlin, Heidelberg, New York, Tokyo

Tyree MT, Yang S (1990) Water-storage capacity of *Thuja*, *Tsuga* and *Acer* stems measured by dehydration isotherms: The contribution of capillary water and cavitation. Planta **182:** 420–426

Waring RH, Whitehead D, Jarvis PG (1979) The contribution of stored water to transpiration in Scots pine. Plant Cell Environ **2:** 309–317